Preparation and Characterization of Magnetic Tips for Magnetic Force Microscopy (MFM) Studies

MASTER THESIS

Author: José Martínez Castro
Director: José María de Teresa Nogueras
University: Universidad de Zaragoza
Master: Nanostructured Materials for Applications in Nanotechnology

Zaragoza, 2012

Contents

Part I
Introduction

Magnetism has been used along the history. Since the invention of the compass and along the years it has become more and more important forming part nowadays of our lifes; in the computers, in every electronic device, in the generation of electricity and other thousand of applications have found that magnetism is at the corel. Magnetism have been studied since long time ago and currently it forms part of a bigger theory called electromagnetism.

Not every metal is capable to create a magnetic field so it is needed a property (a sort of *memory*) called remanence. In normal conditions, only ferromagnetic materials are capable to produce a magnetic field due to its ability to align the magnetic moments in the same direction. The elements with ferromagnetism at room temperature are **Iron, Cobalt, Nickel** and then different kind of alloys.

1 Nanoscience and Magnetism

The number of transistors on integrated circuit doubles approximately over two years. This is the so called Moore's law [1], which has been accomplished for more than four decades. It is been observed that not only referred to transistor but for other components in which this law works properly, for example in the case of hard disk storage cost per unit of information (figure 1).

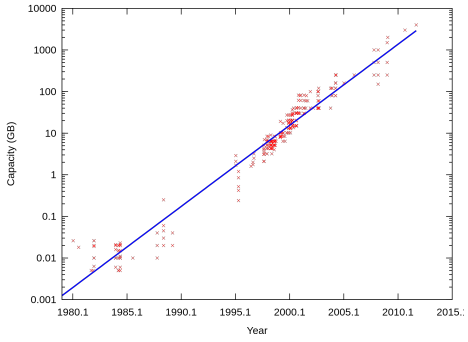

Figure 1: PC hard disk capacity in a logarithmic scale (exponential growth)

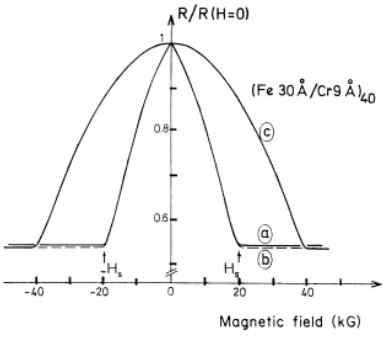

Figure 2: Graph from Fert's article where magnetoresistance of $[(\text{Fe } 30\ \AA)/(\text{Cr } 9\ \AA]_{40}$. Curve a shows the resistance variation when the field is applied in the current direction, curve b perpendicular to the current and curve c perpendicular to the layer plane.

This huge progress could not be possible without the discovery of the giant magnetores-

istance (GMR) by P. Grünberg et al. and simultaneously by A. Fert in 1988 [2].The GMR consist in a significant change in the electrical resistance depending on whether the magnetization of adjacent ferromagnetic layers are in a parallel or an antiparallel alignment (figure 2). As it is seen in the graph, the capacity of information storage has been increasing exponentially. It has been pushing the hard drive industry to improve its technology by decreasing the size of the magnetic domains (without reaching the superparamagnetic limit) with novel compounds and more sophisticated techniques. Since it is not possible to avoid the superparamagnetic limit new ways to store information, related to magnetic systems, are being developed nowadays and for the development different techniques as VSM or Magnetic Field Microscopy has been required for the characterization.

2 Motivation and Steps of the Work

The MFM technique not only depends of the way of measuring chosen, tapping or non contact mode (it will be explained later), but also depends on the selection of the proper tip. A good tip will give us better results in MFM imaging. Nowadays commercial magnetic tips use cobalt for the purpose as in the present work, the major difference is in the fabrication and the thickness of the cobalt layers. These layers have a thickness of 250 nm which causes the creation of a big magnetic field in the tip perturbing the sample.

It is possible to cover AFM tips with a magnetic element (like cobalt) to make them sensitive to the magnetism of the samples, by this method it is possible to cover the tip with different cobalt thickness controlling this way the coercive and the magnetic field of the tip making it more sensitive to magnetic domains and causing a smaller perturbation over the sample.

For this purpose a sputtering machine will be used for covering a commercial AFM tip with Co and a layer of Al to prevent the oxidation. Moreover the characterization of the tip (coercive field) will be done carefully on the different axis of the tip by a sample of a hard disk and an AFM with the MFM implementation which means the possibility of applying a magnetic field in situ. This tips will be used later showing their advantages against commercial tips in MFM studies such as cobalt nanoconstrictions, nanowires of cobalt irradiated with gallium and nickel balls.

3 Characterization Techniques

3.1 Vibrating Sample Magnetometer - VSM

For the purpose of measuring the coercive field and the saturation magnetization on a layer this equipment has been used. The VSM is a type of induction magnetometer (flux method). It consists on two magnets with a uniform magnetic field and a sample vibrating between them (figure 3). The vibration produces a change in the magnetic flux in the

pickup coils and hence an induced voltage (eq. 1) which is proportional to the sample magnetic moment. By this method, measuring in the field of an external electromagnet, it is possible to obtain the hysteresis loop.

$$\varepsilon = -\frac{\partial \phi}{\partial t} \tag{1}$$

The vibration occurs only in one direction so the change on the flux depends by the change in only one direction, the magnetization and the intensity of the applied field.

$$\phi \approx m_m(H,T) K d \cos(\omega t) \tag{2}$$

Where m_m corresponds to the magnetization of the sample, K is a constant, d the amplitude and ω the vibration frequency.
By replacing ϕ in the equation 2, it is possible to obtain the change on the induced voltage with the frequency induced magnetization:

$$V_m = m_m(H,T)\frac{d(Kd\cos(\omega t))}{dt} = m_m(H,T) K d \sin(\omega t) \tag{3}$$

As it is shown on the equation 3, the final dependence will be function of the induced voltage with the frequency ($\sin(\omega t)$), the magnetization of the sample (m_m) and the intensity of the applied field (H).

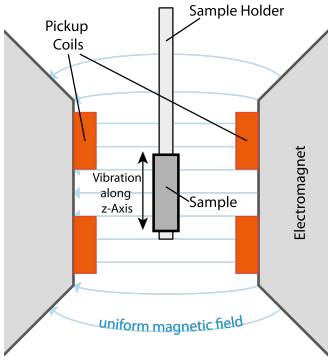

Figure 3: Scheme of a Vibrating Sample Magnetometer

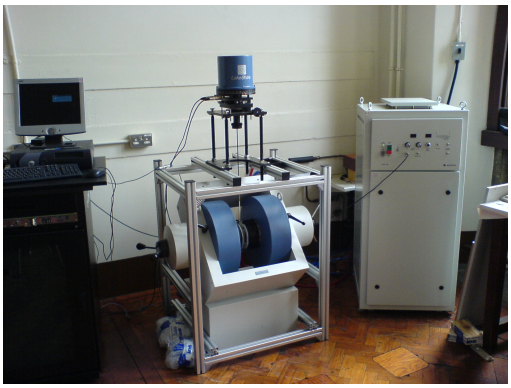

Figure 4: VSM machine

This equipment has a high sensitivity, $10^{-9}V$ which it means up to $10^{-6}e.m.u$ and it is able to apply magnetic fields of 2T. For the present work, VSM placed at INA has been used for the measurements.

3.2 AFM - MFM

The Atomic Force Microscope is a type of microscope included on the scanning probe microscopy. The AFM measures the interaction force between the tip (with the function of probe) and the sample. For the measurement of the force three main characteristics are required:

Force Detector

The Force Detector consists on a cantilever with a very sharp tip mainly fabricated by chemical techniques. The cantilever responses to the Hooke's law (eq. 4) and the normal forces applied to the tip cause a normal deflection of the cantilever.

$$F_N = K_Z \cdot \Delta Z \tag{4}$$

Detection System

The detection Systems use an optical method for the detection of the deflection forces. In the case of conventional AFM's the typical system consists on a photodiode divided in four sectors. The laser beam reflected on the cantilever is picked-up by the photodiode and each sector generates a proportional voltage dependent on the intensity of the light collected.

In the case of advanced AFM systems another methods are used such as the Fabry-Perot cavity, that will be explained later on the *Attocube* section.

Sweeping and Positioning System

A high precision on the positioning of the tip on the sample is needed where the distance is around 1nm. For this purpose piezoelectric systems are used and they are mainly made of piezoelectric ceramics $Pb(Zr_xTi1-x)O_3$. Applying a potential difference between the contacts is possible to contract or expand the piezoelectric with a very high precision in X,Y or Z.

Control Unit

The Control Unit is formed by a high voltage unit linked to a Digital Signal Processor (DSP) and controlled by a computer. The DSP collects and process the signals coming from the photodiode and the control movement from the piezo. It is also responsible for the feedback system which controls the measuring process.

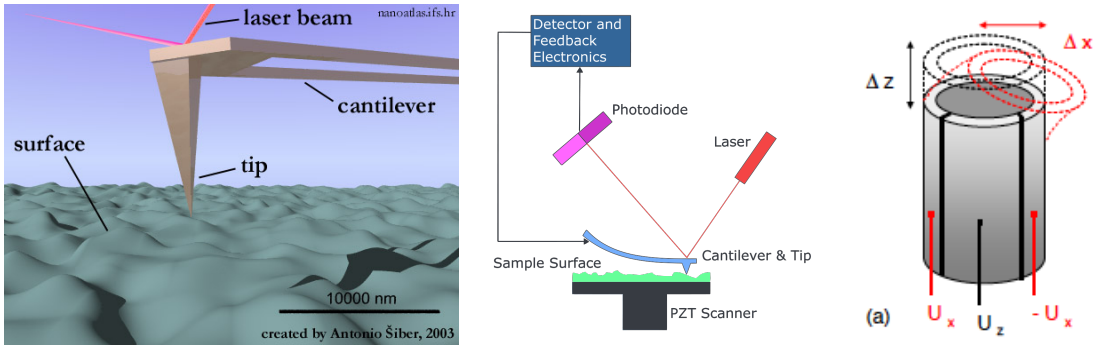

Figure 5: The first image shows the recreation of a cantilever with a tip over a surface. The second image shows how the deflection of the cantilever is detected by the photodiode. The third image shows a typical piezoelectric tube which is able to expand and contract by applying a current.

The magnetic force microscope is an AFM where the tip has been covered with a ferromagnetic material to measure the interaction between the tip and the sample. This microscopy has been widely used since the beginning of nineties, used for its technological applications as a control quality for magnetic devices. Moreover it is still in development improving its resolution and the quantitative interpretation of the data. Three AFM equipments belonging to the LMA (INA) have been used for the research.

3.2.1 Nanotec

The main characteristic of *Nanotec* equipment is the versatility for being modified depending the experiment. One modification that can be done to the equipment is the possibility to add two magnets, capable to apply *out of plane* and *in plane* magnetic fields while the equipment is measuring. For this purpose, the equipment has been designed without any magnetic part except for the magnets.
The *out of plane* magnet consists on a coil over the piezoelectric system where the sample will be located (figure 6). With this system it is only possible to apply magnetic pulses, due to the heating. A field of 700 Oe applied over 30 seconds induces a temperature of 100 °C, hence the system only allows one to apply pulses of 1 s or shorter.
The *in plane* magnet consists on a magnet with a cooling system. The cooling systems allows to apply a magnetic field in a continuous way. It is important to take in account that there is a dependence in the intensity of the field with the distance. The dependence with the temperature was also tested, after a 10 minutes of applying the magnetic field the temperature was only increased in 10 °C.

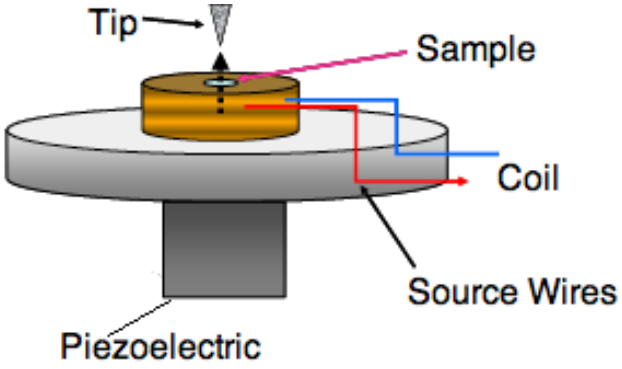

Figure 6: Scheme of the *out of plane* magnet.

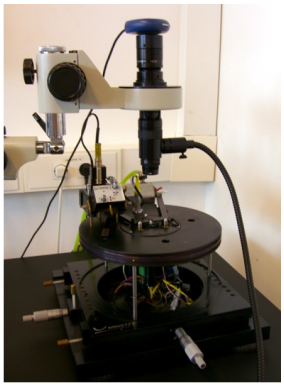

Figure 7: Foto of the equipment used in INA.

3.2.2 Veeco

One of hhe major features of *Veeco* equipment is the mechanical stability: the possibility of changing the tip without perturbing the system and putting it again over the sample very close to the point it was. Moreover *Veeco* is ideal to measure and find different samples in a very short range of time. Beyond these characteristics, it was not the best equipment for MFM measurements because the magnetic parts of the equipment might disturb the measurement besides the lack of magnets for applying magnetic fields in situ.

Figure 8: Picture of an AFM veeco detailing all the parts of the equipment.

Figure 9: Picture of a similar equipment used for the research.

3.2.3 Attocube

Attocube is an SPM equipment specially designed for working on MFM mode at low temperatures. The *Attocube* works as another SPM but having is a big difference in the detection system. In the conventional SPM's, a photodiode picks up the reflected light from the cantilever and in that way the movement of the tip can be detected. When a higher precision is needed, another detection system is required. The detection system is a Fabry-Perot interferometer, typically made of a transparent plate with two reflecting surfaces, or two parallel highly reflecting mirrors. Its transmission spectrum as a function of wavelength exhibits peaks of large transmission corresponding to resonances of the interferometer. The light source is a laser light guided by an optic fiber. When the working point is found in the interferometer, a small change (movement of the cantilever) will produce a considerable variation in the transmission which can be converted into an image with the appropriate software.

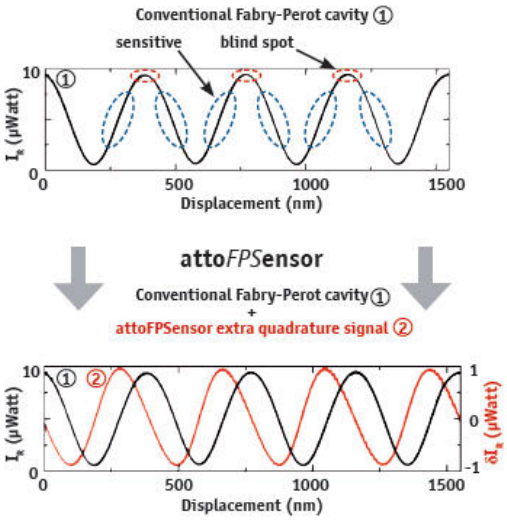

Figure 10: Fabry-Perot cavity.

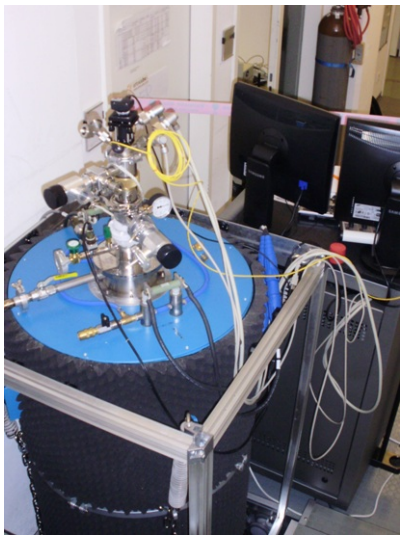

Figure 11: Picture of the equipment used for this research.

The equipment has interesting characteristics that are worth to be mentioned. It is capable to work on non contact mode and in Phase-Locked Loop (PLL) mode. The temperature range can go from 4K to 300 K and it can be even lower depending on the cryostat. The magnetic field reach intensities of 2 T *in plane* and 8 T *out of plane*. The lateral magnetic resolution can be lower than 20 nm with a force gradient detection limit of $0.5\mu N/m$.

Part II
Growth and Characterization of the Samples

4 Sputtering Technique

The Sputtering is a method for the growth of thin layers. It is a relatively simple method where there is a target which is irradiated with ions (in this case, Argon) in order to sputter atoms. Part of these atoms arrive to a substrate, creating in this way thin layers. There are different ways to grow the sample, the chosen one due to its simplicity was growing it with constant pressure and time and quantity of deposited material variable. For the growth of the sample we used the Sputtering Machine placed in INA with a pressure of $6 \cdot 10^{-7}$ Torr and a power of 60 W with an constant Argon pressure of 100 mTorr (which acts as a carrier gas). The sample was covered by a layer of 3 nm of Aluminium to prevent the oxidation of the Cobalt.

Figure 12: Photo of a similar equipment used at INA.

5 Characterization

5.1 Profilometer

To make sure the time of the deposition corresponded to the thickness desired, a profilometer was used. A sample growth by sputtering was chosen to ensure the it had the wanted thickness. The sample was growth pretending to have a thickness of 20 nm and

the profilometer gave us these values: 23; 25,6; 16 and 24,7 nm with an average of 22,3 nm.

5.2 VSM

Hysteresis loops were made for the characterization of the layers with thickness of 10 to 80 nm.

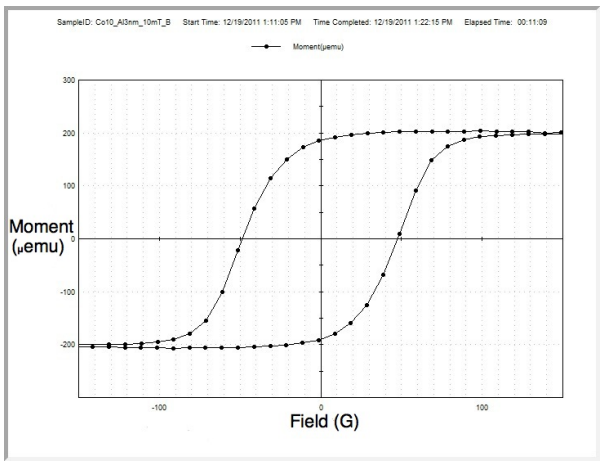

Figure 13: Hysteresis loop for a layer of 10 nm.

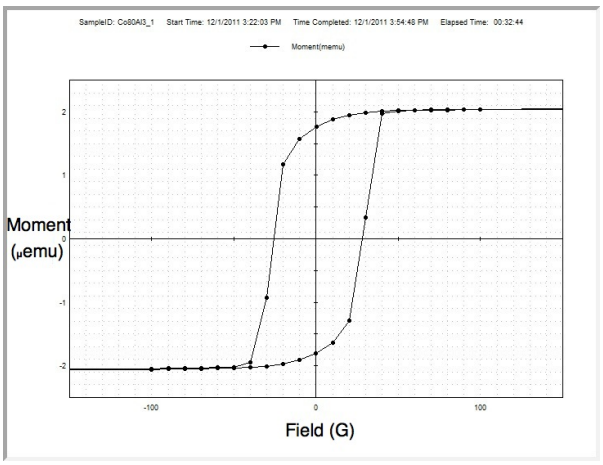

Figure 14: Hysteresis loop for a layer of 80 nm.

From the different graphs it was possible to measure the coercive field of the layers and the saturation magnetization.

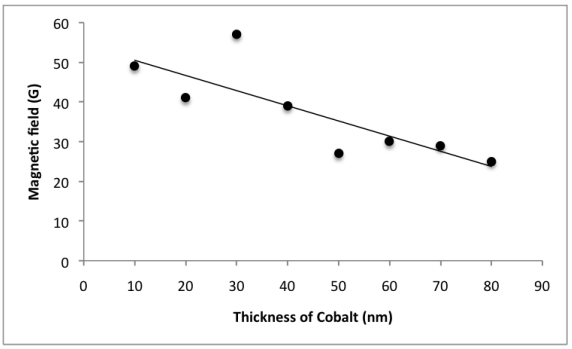

Figure 15: Coercive field of the layers for thickness from 10 to 80 nm.

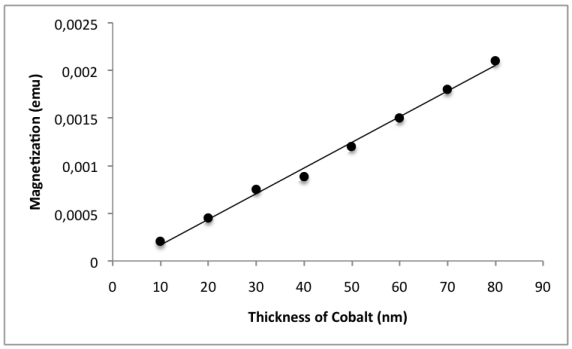

Figure 16: Saturation magnetization of the layers for thickness from 10 to 80 nm.

The saturation magnetization increases with thickness of Cobalt layer (figure 16) as expected from the higher quantity a material. One can notice a decrease on the coercive

field (figure 15) with the increase of the thickness of cobalt. The key to understand this behavior is the **magnetic anisotropy**. The magnetic anisotropy is one of the ingredients for hysteresis in ferromagnets (absence of it means superparamagnetism). Sarathlal K.V et al. [[4]] explain how coercive field can decrease with thickness of Cobalt. As it is shown on the equation 5

$$K_2^{dip} \propto \frac{M_S^2}{D} \tag{5}$$

where, M_S is the saturation magnetization and D is the ferromagnetic film thickness. From the experimental data and the equation can be deduced that with increasing film thickness, the magnetic anisotropy is expected to decrease.

Part III
Characterization of the Tips

6 SEM inside Dual Beam

The SEM images in the Dual Beam of the LMA showed that after the sputtering the covered tips kept their original geometry (pyramidal) and the thickness of Co/Al deposited on the tip corresponded to the thickness for the time deposition on the sputtering machine (20 nm of Co and 3 nm of Al) (figure 17). A gold layer was added to prevent the effects of the electrostatic charge.

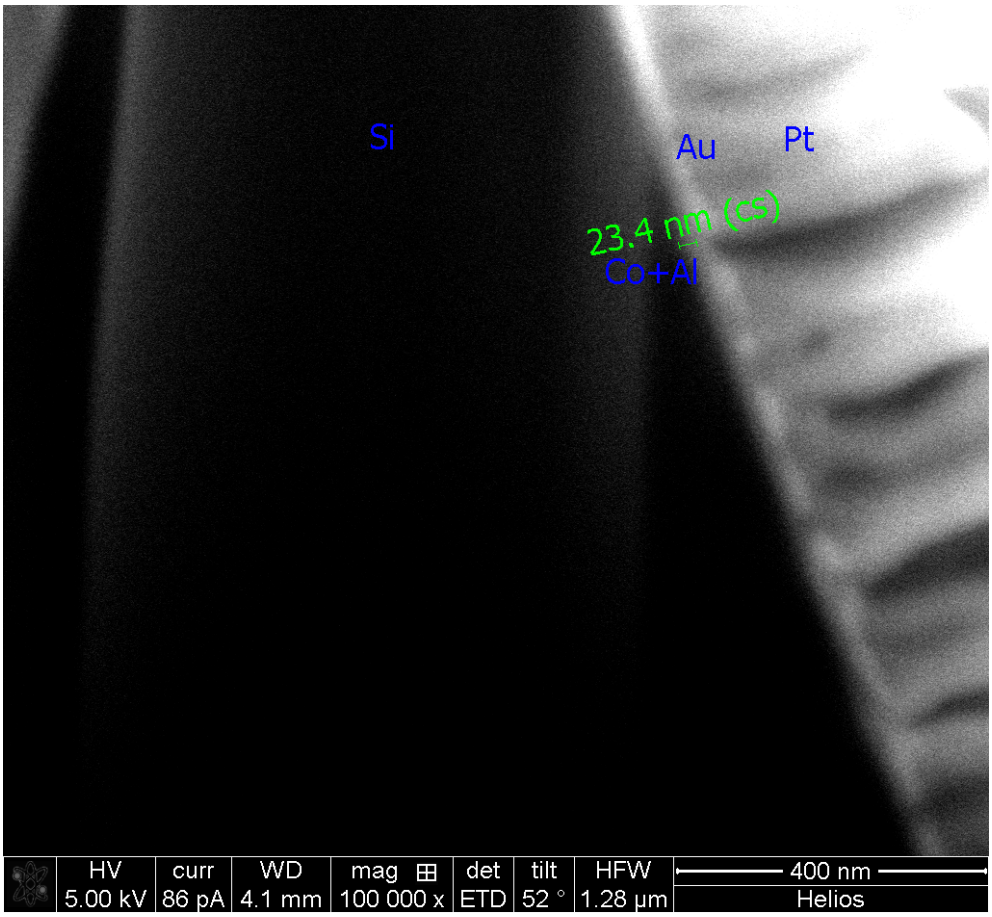

Figure 17: SEM image corresponding to the tip inside the dual beam.

7 MFM

7.1 Theory basics

The SPM techniques are based on the force detection (eq. 6). MFM can be expressed in terms of a convolution of a tip magnetization M_{tip} and the magnetic field crated by the sample H_{sample} (eq. 7).

$$F = \nabla E_{tip-sample} \tag{6}$$

$$E_{tip-sample} \approx \int_{tip} M_{tip} H_{sample} \tag{7}$$

Where integration is performed over the whole magnetic volume of the tip. It can also be assumed that the tip-sample interaction is one-dimensional so considering only the z-components one can obtain an approximated satisfactory results.
There are different ways of detecting the force from a mathematical point of view. The most spread method is the phase shift detection thanks to its proportionality to the force gradient.

$$\Delta\varphi - \frac{Q}{K}\frac{\partial}{\partial z}F_z = -\frac{Q}{K}\frac{\partial^2}{\partial z^2}E_{tip-sample} \tag{8}$$

Where $\Delta\varphi$ corresponds to the phase shift, Q to the charge, and k is a constant [[5]].

7.1.1 Influence of the tip over the samples

Magnetic coatings can be divided into two categories: high coercivity tips like CoCr (or in our case CoAl) and low coercivity (FeNi). Typical coercivity of CoCr are around 400 Oe and low coercivity only about 5 Oe. On the one hand high coercivity on tips may influence the sample magnetic structure but are ideal for applying magnetic fields while measuring, on the other hand low coercivity of the tip does not influence on the sample magnetic domains but those are not suitable for magnetic studies with applied fields in situ. It is worth mentioning that the best way for not changing the sample domains is the non contact mode. With a sample sufficiently smooth it is possible to pass over with a constant height, in this mode the tip travels about 200 nm over the sample. Besides, non contact mode minimizes other forces between the tip and the sample such a Van der Waals forces so it is prefered for MFM measurements.
Another way for measuring magnetic interactions is the tapping mode althought this is not the best mode for MFM technique due to the topography perturbation.
Taking in account that the tips have been covered with CoAl and then tips have high coercivity it is also possible to control the perturbation over the sample by controlling the sweeping speed and the thickness of the cobalt layer.

7.2 Coercive Field Characterization

The tips were characterized on two different ways, on the easy axis, also called out of plane, and on the hard axis of the tip which is called in plane (figure 18).

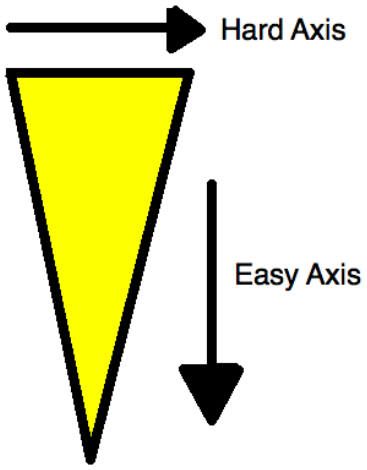

Figure 18: Direction of the easy and the hard axis of the tip.

For this study, the nanotec equipment was employed for its capacity of applying magnetic fields in situ. In the case of *out of plane*, pulsed magnetic fields and in the case of *in plane*, a permanent magnetic field.

7.2.1 Determination of the Coercive Field along Easy Axis of the Tip

The applied magnetic pulses were of less than 1 second long, this is due to the lack of a cooling system of the electromagnet. Anyway the pulse was intense enough to revert the magnetization direction of the tip. Moreover the coercive field could be estimated by applying a progressive field (from -0.15 to 0.15 T and from 0.15 to -0.15 T) and looking into phase shift on the graph. As it is been said before the phase shift is proportional to the force (eq. 8). By keeping the tip in the same position, the only possible explanation to the phase shift is that the magnetic domains of the tip have been reversed by the action of a external magnetic field so the force is exactly the inverse.

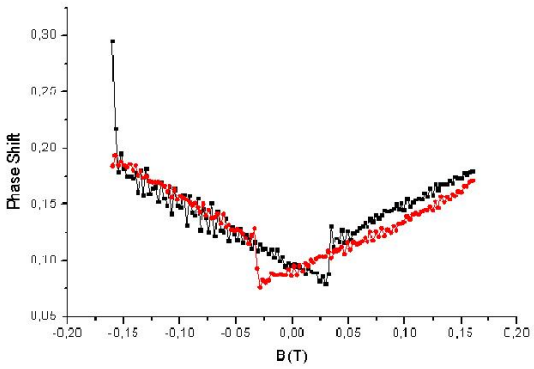

Figure 19: Phase shift diagram for a cobalt thickness of 40 nm.

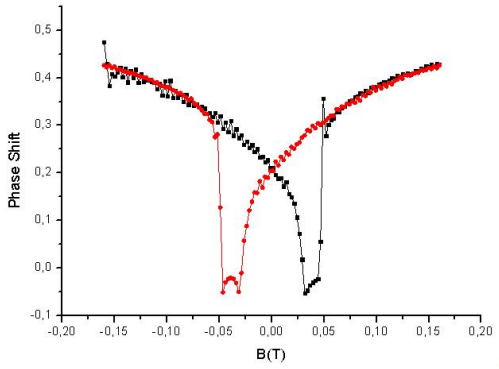

Figure 20: Phase shift diagram for a cobalt thickness of 50 nm.

Once the approximate phase shift was established by the method mentioned before, it was easy to see the change on the magnetic domains. A pulse with the highest magnetic field was applied and then scanned a sample of hard disk, which has a huge coercivity and hence impossible to reverse the magnetization with the applied magnetic fields. Another pulse was applied this time close to the phase shift and another one just after the phase shift. By this method it was possible to see the contrast change(figures 22 and **??**) of the sample caused by the change on the magnetization of the tip.

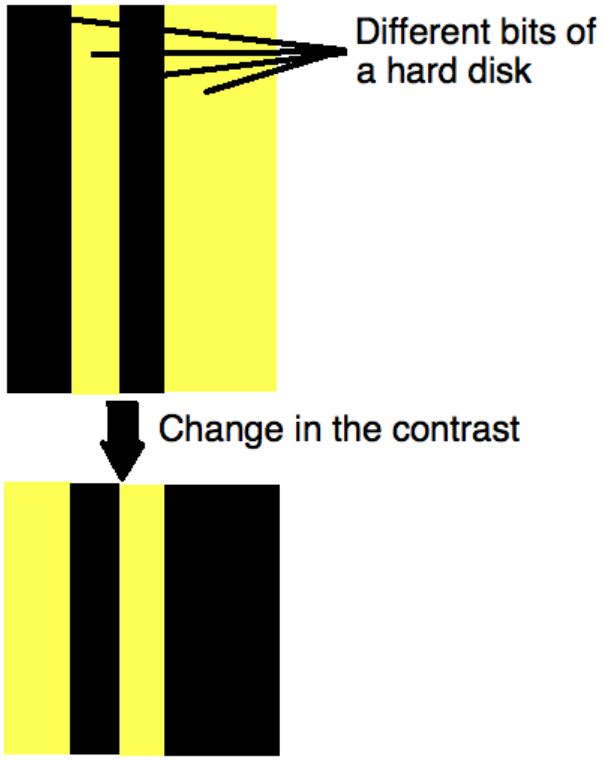

Figure 21: Scheme of the magnetic tracks on a sample of hard disk. The clear area represents a bit a "1" and the dark area a "0". The contrast change turns "0" into "1" and vice versa.

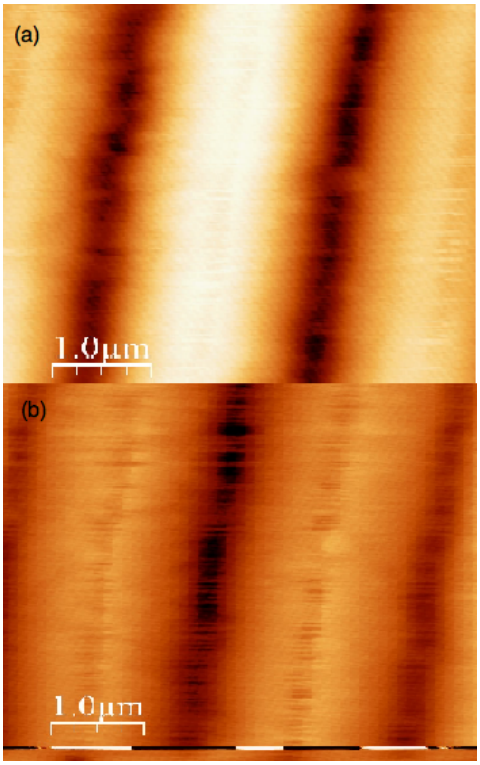

Figure 22: Magnetic images for a sample of hard disk in remanence. (a) With the tip magnetization saturated in one direction, (b) with the tip magnetization saturated in the opposite direction.

Thickness of cobalt	10	20	30	40	50	60	70	80
Coercive field (Oe)	-	500	500	375	425	430	250	300

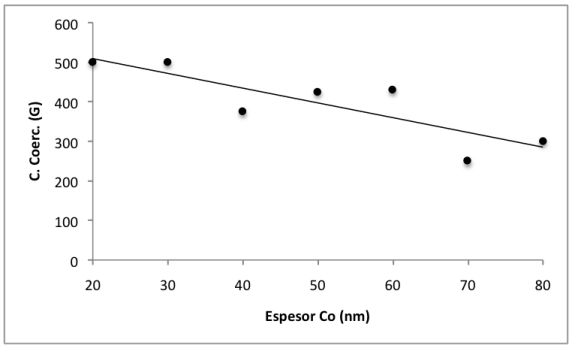

Figure 23: Coercive field for the tips with different thickness of cobalt on the easy axis of the tip. Table and graph.

A tendency to decrease the coercive field can be observed with the increase of cobalt thickness. The dispersion of the data might indicate the thickness of the layer is not the only relevant parameter, but the thickness anysotropy due to the pyramidal shape and imperfections of the fabrication.

7.2.2 Determination of the Coercive Field along Hard Axis of the Tip

In this case a permanent magnetic field was applied to the tip. Such the magnetization on the hard axis is a metastable state it was necessary to apply a permanent field to see the contrast on the case before. On the other hand the phase shift method was not possible to apply due to set up of the experiment. However it was possible to disable *Y scan*, that means scanning in only one line and keep increasing the magnetic field since the change in the contrast was observed (figure 24).

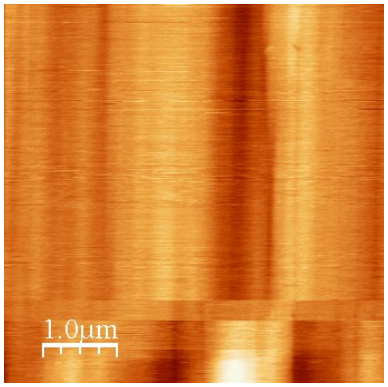

Figure 24: Magnetic contrast change when varying the magnetic field applied to the tip on the hard axis. The y axs indicates the increase in the magnetic field.

Thickness of cobalt	10	20	30	40	50	60	70	80
Coercive field (Oe)	-	1600	1000	1400	1400	1000	1200	1150

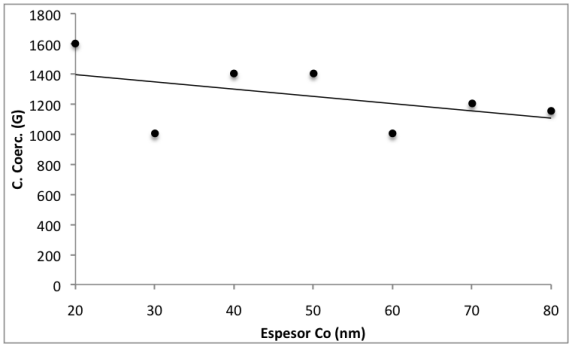

Figure 25: Coercive field for the tips with different thickness of cobalt on the hard axis of the tip. Table and graph.

As in the *out of plane* case it is possible to see a tendency to decrease the coercive field when the increase in the cobalt thickness. However the data scattering points to the anisotropy. By these two studies we can conclude that the values on the easy axis and the hard axis can be delimitated for a tip of CoAl. **[250, 500] and [1000,1600] Oe** for the easy and hard axis respectively. Moreover it can be seen how the coercive field is about four times greater in the hard axis than in the easy axis.
Once the tips have been characterized we proceed to use them in our interest cases.

Part IV
Applications

It is important to clarify that the tips used were those sputtered previously. The tips used were those in the range of 30 to 60 nm thickness. A lower thickness had a poor magnetic interaction and those thicker than 60 nm were too *big* and then the topography was not good enought. For this reason in this range was not so important the thickness but the tips were working properly which means no double tips or imperfections that might have caused a bad image.

8 Cobalt Nanoconstrictions

The studied nanoconstrictions are composed by a cobalt pad and a wire, where the pad is linked to the wire by a constriction of tipically 15 nm thickness [[6]]. The magnetization behavior depends on the sample thickness and the constriction dimensions. And thus, controlling the thickness and hence controlling the magnetization behavior with the applied field it is possible to measure the different magnetoresistance with two electrodes linked to the both sides of the nanoconstriction. The possibility of confine a single domain wall in the constriction area makes possible studies about the structure of the wall and its electrical properties. It could have interesting applications in fields such magnetic storage logic and spin transfer torque applications. For this study Veeco AFM was used; constrictions of different thickness were studied (table 1). The exact dimensions of the constriction were determined by AFM.

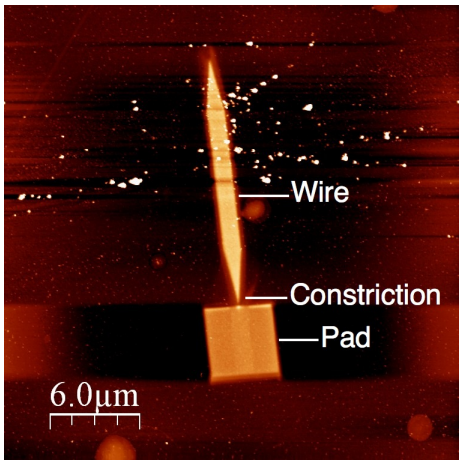

Figure 26: Topographic image of a entire cobalt nanoconstriction detailing all the parts of it.

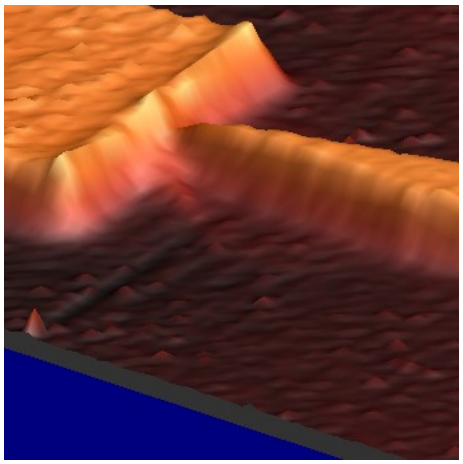

Figure 27: 3D Topographic image of a constriction.

	Const. 1	Const. 2	Const. 3	Const. 4	Const. 5	Const. 6	Const. 7
Wire Thickness (nm)	13	17	20	27	30	35	42
Constriction Thickness (nm)	10	13	14	13	14	16	17
Pad Thickness (nm)	12	17	20	25	27	32	40
Magnetic Image Type	S.D	S.D	D.M.S	L.S	L.S	L.S	L.S

Table 1: Table showing the magnetization structure depending of the type of the pad thickness. S.D is referred to Single Domain, D.M.S to Diamond Multidomain Structure and L.S to Landau Structure.

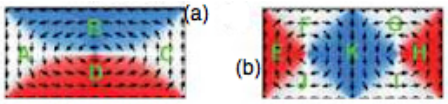

Figure 28: Image corresponding to (a) Landau structure and (b) Diamond structure [[14]].

Two different kinds of structures are shown in remanence depending of the thickness of the pad. Diamond multidomain structure for a thickness of 20 nm (figure 29) and Landau domain structure for pads thicker than 20 nm (figure 31). For pads thinner than 20 nm the image shows single domain structure (figure 33). These states are the most feasible configuration for the thicknesses studied as it is been demonstrated in previous theoretical studies [[6]]. Furthermore a 3D image have been constituted for Landau Structure (figure 32) and for the Diamond Multidomain Structure (figure 30). The difference in height in the images represent the different orientation of the magnetic domains of the pads. It can be seen that the Diamond Multidomain Structure is a much more complicated state than the Landau Structure.

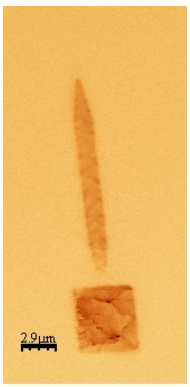

Figure 29: Magnetic image for a pad of 20 nm thickness.

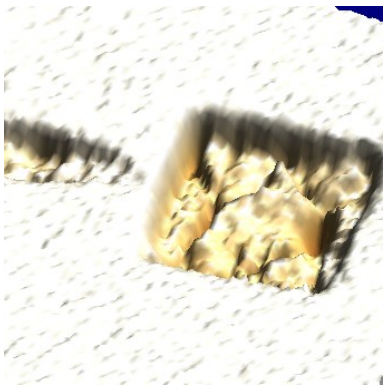

Figure 30: 3D Magnetic image of a constriction of 20 nm thickness.

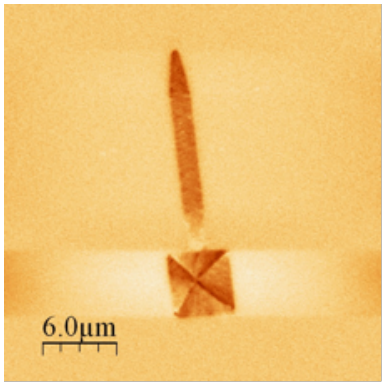

Figure 31: Magnetic image for a pad of 32 nm thickness.

Figure 32: 3D Magnetic image of a constriction of 32 nm thickness.

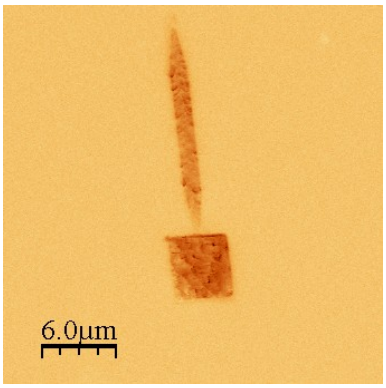

Figure 33: Magnetic image for a pad of 17 nm thickness.

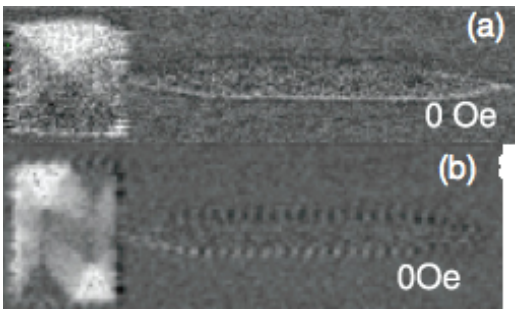

Figure 34: Images of cobalt nanoconstrictions obtained by STXM of a Landau domain wall (a) and a Diamond multidomain wall both in remanence (b) (A. Fernandez-Pacheco et al. [[6]]).

In this study has been possible to obtain the same results than in the study performed by A. Fernandez-Pacheco et al. [[6]] by STXM technique (figure 34) as it has been shown in the previous images. Unfortunately it has not been possible to observe the magnetic state of the constriction due to its small size and the experimental difficulties.

9 Cobalt Wires Irradiated with Gallium Focused Ion Beam

The purpose of this study is to see how the domain walls change with the irradiation of Gallium. Magnetic fields have been applied in situ to change the magnetization of the wires and measure them in remanence. By the change on the contrast it was possible to discern which kind of magnetic contribution was coming from the wire and which one from the tip.
A detailed explanation for the understanding of the magnetic images is required. The different aspects to take in account are: the electrostatic contribution in the final image, the shape of the domain walls and the influence of the Gallium irradiation to the width of the domain walls.

Domain Wall Shape.
From a fundamental physical point of view, the domain-wall types result from a minimization of the energetics governing the magnetization configurations in small magnetic structures (exchange, magnetostatic, and anisotropy). There are fundamentally three types of domain walls depending on the thickness. Transverse wall, asymmetric transverse wall and vortex wall (*Joonyong Kim et al.* [[8]]) (figure **??**). The appearance of the different domain walls depends on the thickness and the width of the nanowire. In the study previously cited, wires of 10 nm thickness, transverse wall become stable, whereas for 20 nm asymmetric transverse wall are observed. This is a metastable phase between transverse and vortex wall. For wires thicker than 40 nm vortex wall are observed since it has much smaller magnetostatic energy than the other types which are only stable when there is a small exchange energy. As it is mentioned before not only thickness is important but also the width for the formation of the domain walls. *Kläui et al.* [[9]] showed that there is a limit in width and thickness for the appearing of the vortex domain in Cobalt rings (figure 36).

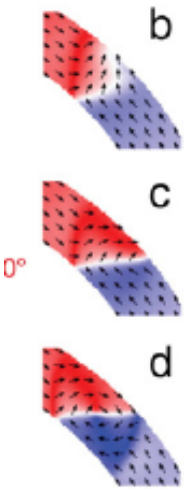

Figure 35: (b) Transverse wall, (c) Asymmetric transverse wall and (d) Vortex wall (Klaui et al. [[9]]).

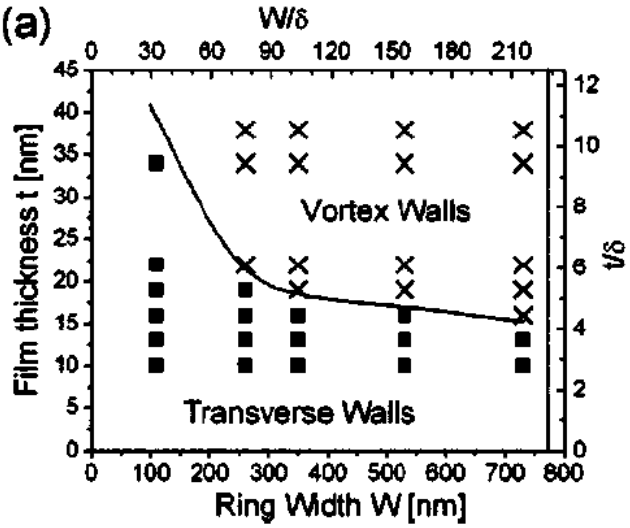

Figure 36: Experimental phase diagram for polycrystalline Co rings (Klaui et al. [[9]]).

Electrostatic Contribution.

One of the major problems when MFM imaging is the electrostatic contribution. Van der Waals forces are easy to avoid by lifting up the tip a few tens of nanometers (the so called lift mode) but the electrostatic are in the same range as the magnetic contribution. A few studies have been done reporting and trying to solve this problem and one way to solve it is by the Kelvin Probe Force Microscopy (KPFM). By this method it is possible to remove the electrostatic contribution on the interaction tip-sample and then having a better resolution on the magnetic image.

KPFM is a method where the potential offset can be measured between the probe tip and the surface can be measured. An alternate current is applied at the cantilever which is the resonance frequency. When a direct current is applied to the cantilever (electrostatic interaction tip-sample) it causes the perturbation of the cantilever varying the frequency vibration that can be measured.

A combination of MFM and KPFM is possible as implemented by the group of Agustina Asenjo [[3]]. By this technique it is possible to subtract the electrostatic contribution and have a clearer magnetic image, as it was recently demonstrated on similar samples to the ones studied here [[10]].

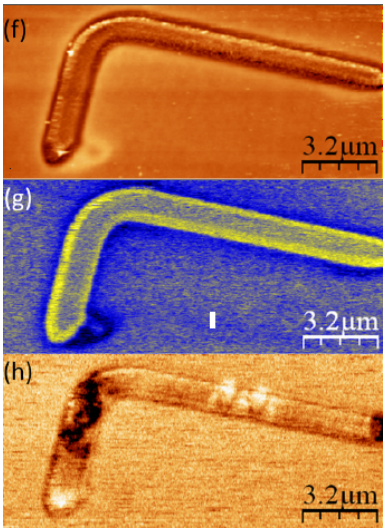

Figure 37: (f) Magnetic image without applying the KPFM technique, (g) Electrical contribution by only measuring with KPFM technique, (h) Final image where MFM and KPFM have been applied at the same time (M. Jaafar et al. [[10]]).

In the final image it is possible to see the magnetic domains (vortex type) in the middle of the L-shape cobalt nanowire.

Influence of Gallium Irradiation over the Cobalt Wires.
The equation that governs the domain wall width is:

$$\Delta = \pi\sqrt{A/K} \tag{9}$$

where Δ is the domain wall width, A the exchange stiffness and K the magnetic anisotropy. In systems with a strong perpendicular anysotropy it has been demonstrated that the anysotropic constant decreases with Ga irradiation, thus changing the DW width [[7]]. Our targe is to investigate if changes are produced on domain walls width on Co nanowires irradiated with Ga.

Cobalt nanowires have been measured with Nanotec and Veeco equipment. The advantage of Nanotec is the capacity for applying magnetic fields in situ. By the application of the magnetic fields it is possible to distinguish magnetic contributions on the image from topographic, electrostatic or another kind of contribution due to the fact there is a contrast change (white turns into black and black turns into white) (figure 39).

Figure 38: The circles show the magnetic flux coming in and out due to the single-domain state existing in this wire. The other contrast changes are produced by the topography.

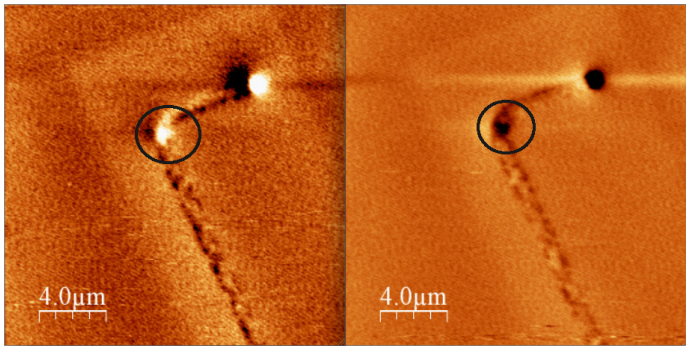

Figure 39: Contrast change for the same nanowire by applying opposite magnetic fields and measuring it in remanence.

Moreover it was possible to distinguish the vortex wall on Co nanowires in the corner. The anisotropy of the L-Shape helps the formation of these structures in the corner (Eq. 9). In the other side it was impossible to measure a increase or decrease in the size of the domain walls. This is caused to the fact that the vortex walls become blurry, probably to the action of the electrostatic forces which can mask the magnetic interaction. As a conclusion it can be said that it is possible to appreciate the vortex walls on the corner of the wires but it is not possible to measure them due the tip-sample electrostatic interaction. One way to solve this problem would be to apply the Kelvin Probe Force Microscopy at the same time when measuring and subtract this information to obtain a clear magnetic image of the Co nanowires.

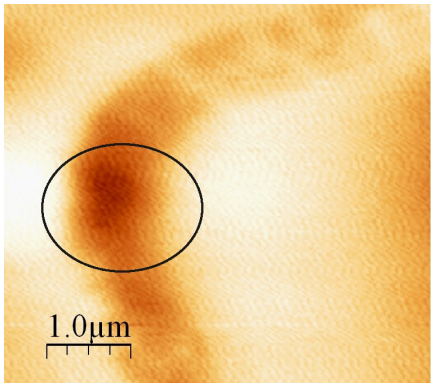

Figure 40: The electrostatic interaction between sample-tip make the resulting image of the domain wall blurry and impossible to measure the type of wall and the change on the size. .

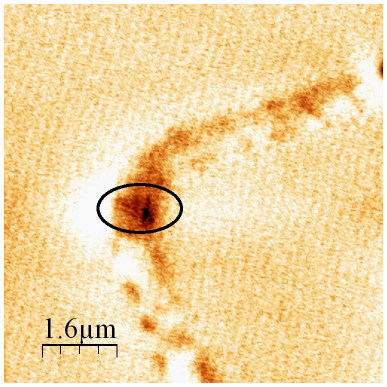

Figure 41: Domain wall can be clearly seen in the image as a typical triangle shape.

Measurements of Co nanowires were performed with Veeco equipment. The idea was, thanks to the optimized software, to have better resolution images. However, no good magnetic images were found (figure 42), in part for the incapacity of applying magnetic fields in situ.

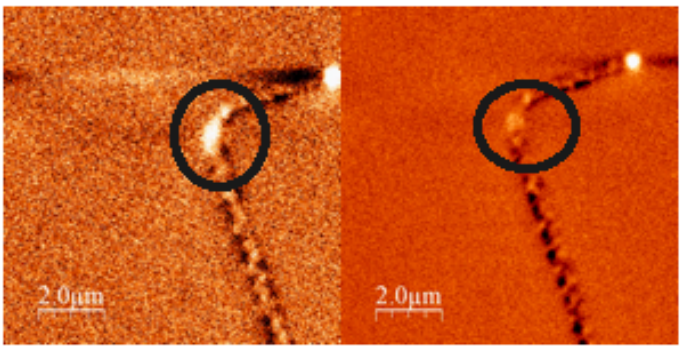

Figure 42: Co nanowires magnetic images obtained with Veeco equipment.

To demonstrate that home-made tips were working properly, measurements with a commercial tip were performed (figure 43). As it can be seen on the image, the field created by the tip is so high that it perturbs the magnetic image of the wire.

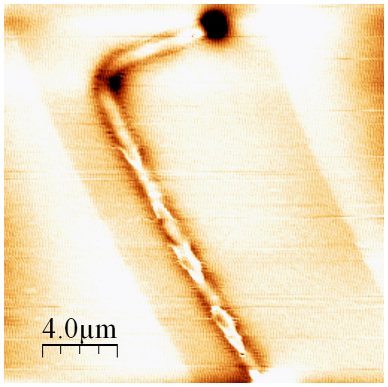

Figure 43: Co nanowire image obtained with a commercial tip.

10 Remanent Fields of Nickel Balls

The evolution of dewetting in nanoscopic metal films has been investigated [[11]], [[12]]. For the formation of the nickel balls array dewetting was performed by pulsed laser melting. Dewetting depends on film thickness, laser enery density and laser irradiation time. It has been observed that the formation of nanoparticles depends on time of irradiation, since short pulses form polygons, longer pulses cause the formation of the nanoparticles. More recently, pulsed laser dewetting of nickel has been investigated [[13]], observing the same behavior as in other metal films, creating a nanoparticle after 100 pulses of 25 ns with a Kripton Fluoride laser which has a frequency of 248 nm and adjusting the laser fluence for the purpose.

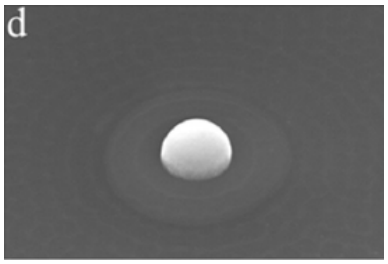

Figure 44: Nickel dewetting after receiving 100 pulses of 0.42 $J \cdot cm^{-2}$ [[13]].

Nickel balls (NB) have interesting applications as a catalysts and also in magnetic devices due to the ferromagnetic behavior. In this study different arrays of NB was created with different balls separation between them. The samples were grown by Jason Fowlkes. The SEM and MOKE characterization of these samples before the present work are shown here (figure 45, 46, 47).

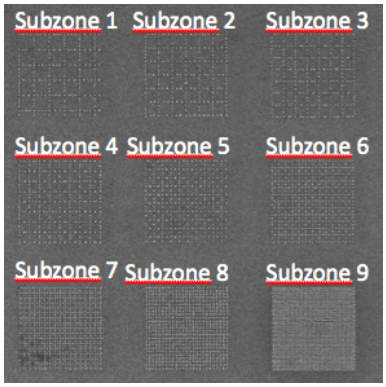

Figure 45: Sample with different array patterings.

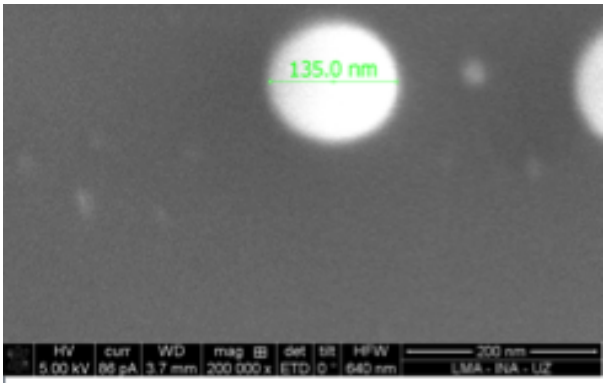

Figure 46: Single NB of 135 nm.

The diameter of the NB oscillates between 120 and 140 nm with a Ni content of 60 - 75%. A MOKE study was performed for the NB's; the hysteresis loop shows the ferromagnetism of the NB (figure 47). However a more detailed study was necessary since is necessary a detailed study of the ferromagnetism of a single NB and not only for the whole sample.

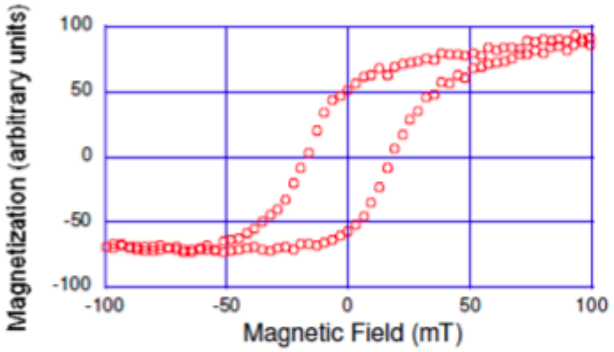

Figure 47: Hysteresis loop perfomed by MOKE of an array of NB's.

The MFM measurement of NB's were made by Veeco equipment due to its stability and ease to find the required sample. As it is been said before, Veeco equipment is not capable of applying magnetic fields in situ. The sample was magnetized ex-situ and then the tip was also magnetized in opposite directions on the easy axis to appreciate the contrast change on the Ni balls. To ensure that the field created by the tip was not affecting the magnetization of the NB, the sample was magnetized on plane and it was meaured at 0 and 90 were done. If the Ni balls had been affected by the tip then the same image would have been observed. In the other hand different images were observed,

showing that the nickel balls were not affected by the tip (figures 48 and 49). When the measurement changed from 0 to 90 degrees, as it can been oberved in the picture, the black contrast rotated 90º changing from the left side to the down part of the NB's. In contrast, a commercial tip would have probably affected the magnetization of the NB's because of its higher magnetic field making impossible to measure remanent fields on Nickel Balls.

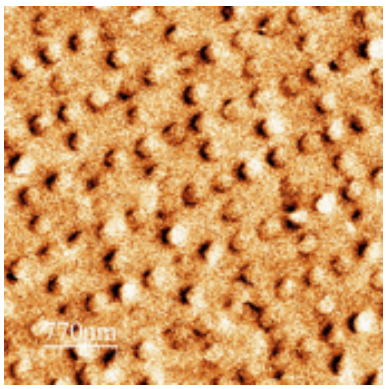

Figure 48: Magnetization of the NB's at 0 degrees.

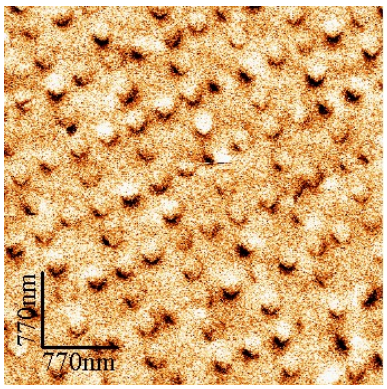

Figure 49: Magnetization of the NB's at 90 degrees.

Once it was sure the tip was not affecting the magnetization of the NB's, the magnetization of the tip was changed on the easy axis of the tip (figures 50 and 51).

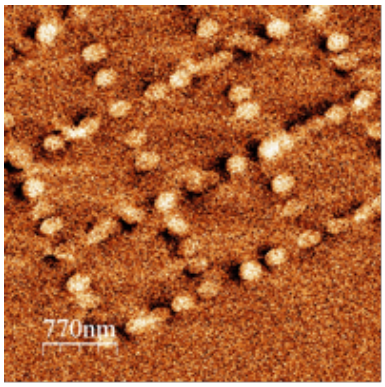

Figure 50: Tip magnetized in a direction on the easy axis

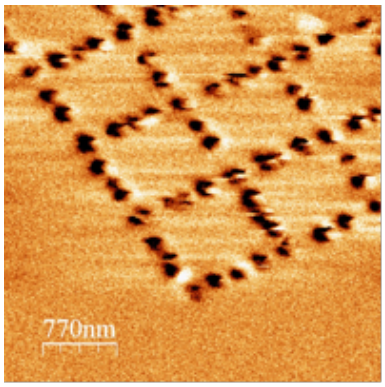

Figure 51: Tip magnetized on the opposite direction on the easy axis.

As it can be seen the contrast on the NB's change by changing the magnetization direction of the tip from white to black. It demonstrates that each NB is ferromagnetic.

Part V
Conclusion and Acknowledgements

11 Conclusion

This Final Master Project has been focused on the characterization of the magnetic tips and their applications. As it has been demonstrated, the coercive field of the magnetic tips decrease with the thickness increase of the cobalt layer in the easy and the hard axis of the tip. Besides this general tend, an an extrinsic contribution has been observed, the shape of the tips cause probably an irregular deposition when they are being sputtered which causes a difference in the coercive field with only a difference of 10 nm. Another conclusion is that coercive field of the easy and the hard axis of the tip can be delimited between two values [250 ,500] and [1000, 1600] Oe. A final conclusion about the characterization of the tips is that any tip which has been sputtered should be characterized before the magnetic study that should be used for.

Three different studies have been performed with the sputtered tips:
A MFM study has been done over constrictions. This study has shown (as previously in other studies) that depending of the thickness of the pad, different magnetic domain shapes can exist like Landau Structure for pads thicker than 20 nm, Diamond Multidomain Structure for pads of 20 nm thick and single magnetic domains for pads thinner than 20 nm.

Cobalt nanowires have shown that it is possible to see the domain walls over the corner, however, the noise, like the electrostatical interaction or the influence of the tip over the sample makes that the increase or decrease of the domain wall size could not be measured by this technique neither in *Nanotec* or *Veeco* equipment neither the domain wall shape as well. A proper measurement with a commercial tip was made showing that those tips are not good enough when an accurate measurement is required probably due to the high magnetic field created by tip which masks all the magnetic signal coming from the nanowire.
A last study was performed over Nickel Balls. The main objective was to discern if the NB's had ferromagnetic properties and hence the magnetic domain for each ball. It was demonstrated that the nickel balls were ferromagnetic and the tip was not affecting the NB's by changing the sweeping angle from 0 to 90 degrees and after that, by changing the tip orientation on the easy axis, observing a change in the NB's contrast from white to back.

12 Acknowledgements

The author of this Final Master Project acknowledges support from the Institute of Nanoscience of Aragon and the collaboration and help on this project of the following persons: Luis Enrique Serrano Ramón for his help in different aspects such as theoretical background, Dual Beam equipments and AFM equipments. Jose Luís Díez for his help as a technician of AFM equipments. Pavel Strichovanec for his help on sample growth on the sputtering technique and VSM measurements. David Serrate for his help on the *Attocube* equipment.

References

[1] *Moore, Gordon E.* Cramming more components onto integrated circuits, 1965, Electronics Magazine. p. 4. Retrieved 2006-11-11.

[2] *P. Grünberg et al.* Giant Magnetoresistance of (001)Fe/(001)Cr Magnetic Superlattices, 1988, Physics R. Letters. Volume 61, Number 21.

[3] *Miriam Jaafar Ruiz – Castellanos.* Procesos de imanación en la nanoescala mediante microscopía de fuerzas magnéticas, February 2009, Universidad Autónoma de Madrid.

[4] *Sarathlal K.V. et al.* In-situ study of magnetic thin films on nanorippled Si (1 0 0) substrates, August 2011, Applied Surface Science 258, 4116– 4121.

[5] *SPMTIPS.* Characterization and calibration of MFM tip. Quantitative measurements in Magnetic Force Microscopy ($http : //www.ece.nus.edu.sg/stfpage/elewuyh/News/mfm_cali.pdf$).

[6] *A. Fernández-Pacheco et al.* Correlation between the magnetic imaging of cobalt nanoconstrictions and their magnetoresistance response, 2012, Nanotechnology 23, 105703.

[7] *J. H. Franken et al.* Tunable Resistivity of Individual Magnetic Domain Walls, January 2012, Physical Review Letters, PRL 108, 037205.

[8] *Joonyong Kim et al.* Domain wall types and field-induced domain wall motion in L-shaped nanowires, April 2011, Thin Solid Films, 519 8263–8265.

[9] *M. Kläui et al.* Head-to-head domain-wall phase diagram in mesoscopic ring magnets, Dicember 2004, Applied Physics Letters, 85, 5637.

[10] *M. Jaafar et al.* Distinguishing magnetic and electrostatic interactions by a Kelvin probe force microscopy–magnetic force microscopy combination, September 2011, Beilstein J. Nanotechnol., 2, 552–560.

[11] *C. Favazza et al.* Robust nanopatterning by laser-induced dewetting of metal nanofilms, 2006, Nanotechnology, 17, 4229–4234.

[12] *J. Trice et al.* Pulsed-laser-induced dewetting in nanoscopic metal films: Theory and experiments, 2007, Physical Review B, 75, 235439.

[13] *Y. F. Guan et al.* Pulsed laser dewetting of nickel catalyst for carbon nanofiber growth, 2008, Nanotechnology, 19, 235604.

[14] *Kaixuan Xie et al.* Magnetization splitting in Landau and diamond-domain structures: Dependence on exchange interaction, anisotropy, and size, August 2011, Phys. Rev. B 84, 054460.